Journal of Applied and Computational Mechanics, Vol. 2, No. 4, (2016), 254-261
DOI: 10.22055/JACM.2016.12545

Journal of
Applied and Computational Mechanics

Dynamic Buckling of Embedded Laminated Nanocomposite Plates Based on Sinusoidal Shear Deformation Theory

Mohammd Sharif Zarei[1], Mohammad Hadi Hajmohammad[2,*], Ali Nouri[2]

[1]Faculty of Engineering, Ayatollah Boroujerdi University, Boroujerd, Iran
[2]Department of mechanical engineering, Imam hossein University, Tehran, Iran

Received December 2 2016; revised January 1 2017; accepted for publication January 2 2017.
Corresponding author: Mohammad Hadi Hajmohammad, hadi.hajmohammad@gmail.com

Abstract

In this study, the dynamic buckling of the embedded laminated nanocomposite plates is investigated. The plates are reinforced with the single-walled carbon nanotubes (SWCNTs), and the Mori-Tanaka model is applied to obtain the equivalent material properties of them. Based on the sinusoidal shear deformation theory (SSDT), the motion equations are derived using the energy method and Hamilton's principle. The Navier's method is used in conjunction with the Bolotin's method for obtaining the dynamic instability region (DIR) of the structure. The effects of different parameters such as the volume percentage of SWCNTs, the number and orientation angle of the layers, the elastic medium, and the geometrical parameters of the plates are shown on DIR of the structure. Results indicate that by increasing the volume percentage of SWCNTs the resonance frequency increases, and DIR shifts to right. Moreover, it is found that the present results are in good agreement with the previous researches.

Keywords: Dynamic buckling, Nanocomposite laminated plates, Elastic medium, SSDT, Bolotin's method.

1. Introduction

The stiff, strong, and lightweight composite materials are being widely used in many structural members, such as the multilayered composite plates. The laminated composite structures are made up of the layers of orthotropic materials that are bonded together, whereas the sandwich structures consist of a thick and light core surrounded by the face sheets which possess high strength and high stiffness, thereby increasing the resistance to bending. The dynamic stability problems which have attracted the attention of many researchers up to the present are still among the most important problems for the laminated composite plates.

Many researches have been done on the mechanical analysis of the laminated plates. The natural frequencies and the buckling stresses of the cross-ply laminated composite plates were analyzed by Matsunaga [1] taking into account the effects of the shear deformation, thickness change, and rotatory inertia. The dynamic behavior of the laminated composite plates undergoing moderately large deflection was investigated by Kim and Kim [2] considering the viscoelastic properties of the material. In order to accurately determine the dynamic response of the cross-ply laminated thick plates subjected to a moving load, a solution procedure was presented based on the three-dimensional (3D) elasticity theory by Malekzadeh et al. [3]. The natural neighbour radial point interpolation method (NNRPIM), an improved meshless method, was used by Dinis et al. [4] in the numerical implementation of an unconstrained third-order plate theory which was applied to the laminates. Honda et al. [5] extended the layerwise optimization (LO) procedure to the maximization problem of the fundamental frequencies of the sandwich plates with the fibrous composites and low stiffness core layers. A new inverse trigonometric zigzag theory was proposed by Sahoo and Singhand [6] which was implemented for the static analysis of a laminated composite and the sandwich plates. Heydari et al. [7] presented an analytical approach for the transverse bending analysis of an

embedded symmetric laminated rectangular plate using the Mindlin plate theory. In this study the surrounding elastic medium was simulated using the Pasternak foundation. A simple hyperbolic shear deformation theory which took into account the transverse shear deformation effects was proposed by Saidi et al. (8) for the free flexural vibration analysis of the thick functionally graded plates resting on elastic foundations. A method for studying the dynamical instability and non-linear parametric vibrations of the symmetrically laminated plates of complex shapes having different cutouts was proposed by Awrejcewicz et al. [9]. Liang [10] extended the Koiter–Newton method for the nonlinear buckling analysis of the thick and thin laminated composite plates.

To the best of our knowledge, the dynamic buckling analyses of the sandwich nanocomposite plates have not received enough attentions so far. Motivated by these considerations, the purpose of this study is to investigate the dynamic buckling analysis of the nanocomposite laminated plates resting on an elastic medium based on SSDT in order to optimize the sandwich structures. The elastic medium is simulated with the orthotropic Pasternak medium. The Navier and Bolotin methods are applied to obtain the dynamic instability region of the system. To validate the work, the results are compared with those reported in the literature. The effects of different parameters such as the volume percentage of SWCNTs, the number and orientation angle of the layers, the elastic medium, and the geometrical parameters of the plates are shown on DIR of the structure.

2. SSDT

A schematic figure of the laminated plates with the nanocomposite layers is shown in Fig. 1with the Cartesian coordinate system (x, y, z) which is used in the middle layer of the nanocomposite where the thickness coordinate z ranges from $-h$ to $+h$. As can be seen in this figure, the length and width of the plates are a and b, respectively. The elastic medium is simulated by the spring and shear layers.

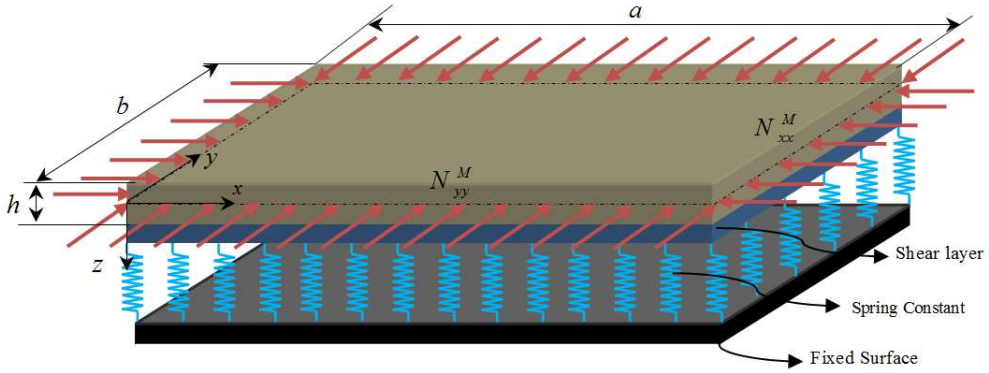

Fig. 1. The embedded laminated plate with SWCNTs-reinforced layers

Based on SSDT, we have [11]

$$u_1(x,y,z,t) = u(x,y,t) - z\frac{\partial w}{\partial x} + \frac{2h}{\pi}\sin(\frac{\pi z}{2h})\varphi_x \ , \tag{1}$$

$$u_2(x,y,z,t) = v(x,y,t) - z\frac{\partial w}{\partial y} + \frac{2h}{\pi}\sin(\frac{\pi z}{2h})\varphi_y \ , \tag{2}$$

$$u_3(x,y,z,t) = w(x,y,t) + \cos(\frac{\pi z}{2h})\varphi(x,y,t) \ , \tag{3}$$

where u, v, and w are the displacements of the mid-plane along the axes x, y, and z, respectively, and φ_x, φ_y, and φ are the rotations about the y, x, and z axes and account for the effects of the transverse shear. According to the reference [38], further assumptions can be written as:

$$w(\mathrm{x},\mathrm{y},\mathrm{t}) = w_b(\mathrm{x},\mathrm{y},\mathrm{t}) + w_s(\mathrm{x},\mathrm{y},\mathrm{t}), \tag{4}$$

$$\varphi_x = \frac{\partial w_s}{\partial x}, \tag{5}$$

$$\varphi_y = \frac{\partial w_s}{\partial y}. \tag{6}$$

Based on the displacement field of the quasi-3D SSDPT, the in-plane and the transverse shear strains of each layer may be expressed as:

$$\varepsilon_{xx} = \frac{\partial u}{\partial x} + \frac{1}{2}(\frac{\partial w_b}{\partial x} + \frac{\partial w_s}{\partial x} + \mathrm{g(z)}\frac{\partial \varphi}{\partial x})^2 - z\frac{\partial^2 w_b}{\partial x^2} - f(\mathrm{z})\frac{\partial^2 w_s}{\partial x^2}, \tag{7}$$

$$\varepsilon_{yy} = \frac{\partial v}{\partial y} + \frac{1}{2}(\frac{\partial w_b}{\partial y} + \frac{\partial w_s}{\partial y} + \mathrm{g(z)}\frac{\partial \varphi}{\partial y})^2 - z\frac{\partial^2 w_b}{\partial y^2} - f(\mathrm{z})\frac{\partial^2 w_s}{\partial y^2}, \tag{8}$$

$$\varepsilon_{zz} = g'(\mathrm{z})\varphi, \tag{9}$$

$$\gamma_{xy} = \frac{\partial u}{\partial y} + \frac{\partial v}{\partial x} + (\frac{\partial w_b}{\partial x} + \frac{\partial w_s}{\partial x} + \mathrm{g(z)}\frac{\partial \varphi}{\partial x})(\frac{\partial w_b}{\partial y} + \frac{\partial w_s}{\partial y} + \mathrm{g(z)}\frac{\partial \varphi}{\partial y}) - 2z\ \frac{\partial^2 w_b}{\partial y\,\partial x} - 2f\ (\mathrm{z})\frac{\partial^2 w_s}{\partial x^2}, \tag{10}$$

$$\gamma_{xz} = g\,(\mathrm{z})\left(\frac{\partial w_s}{\partial x} + \frac{\partial \varphi}{\partial x}\right), \tag{11}$$

$$\gamma_{yz} = g\,(\mathrm{z})\left(\frac{\partial w_s}{\partial y} + \frac{\partial \varphi}{\partial y}\right), \tag{12}$$

where $f\ (\mathrm{z}) = \mathrm{z} - \frac{h}{\pi}\sin\left(\frac{\pi z}{h}\right)$ and $g\ (\mathrm{z}) = \cos\left(\frac{\pi z}{h}\right)$.

The constitutive equation for the stresses σ and the strains ε matrix of the kth layer can be expressed as follows [12]:

$$\begin{Bmatrix} \sigma_{xx} \\ \sigma_{yy} \\ \sigma_{xy} \\ \sigma_{xz} \\ \sigma_{yz} \end{Bmatrix}^{(\mathrm{k})} = \begin{bmatrix} Q_{11} & Q_{12} & Q_{16} & 0 & 0 \\ Q_{12} & Q_{22} & Q_{26} & 0 & 0 \\ Q_{16} & Q_{26} & Q_{66} & 0 & 0 \\ 0 & 0 & 0 & Q_{55} & Q_{45} \\ 0 & 0 & 0 & Q_{45} & Q_{44} \end{bmatrix}^{(\mathrm{k})} \begin{Bmatrix} \varepsilon_{xx} \\ \varepsilon_{yy} \\ \gamma_{xy} \\ \gamma_{xz} \\ \gamma_{yz} \end{Bmatrix}^{(\mathrm{k})}, \tag{13}$$

where $Q_{ij}\ (i, j = 1,2,...,6)$ can be defined as:

$$Q_{11} = C_{11}\cos^4\theta - 4C_{16}\cos^3\theta\sin\theta + 2\left(C_{12} + 2C_{66}\right)\cos^2\theta\sin^2\theta - 4C_{26}\cos\theta\sin^3\theta + C_{22}\sin^4\theta, \tag{14a}$$

$$Q_{12} = C_{12}\cos^4\theta + 2\left(C_{16} - C_{26}\right)\cos^3\theta\sin\theta + \left(C_{11} + C_{22} - 4C_{66}\right)\cos^2\theta\sin^2\theta + 2\left(C_{26} - C_{16}\right)\cos\theta\sin^3\theta + C_{12}\sin^4\theta, \tag{14b}$$

$$Q_{16} = C_{16}\cos^4\theta + \left(C_{11} - C_{12} - 2C_{66}\right)\cos^3\theta\sin\theta + 3\left(C_{26} - C_{16}\right)\cos^2\theta\sin^2\theta + \left(2C_{66} + C_{12} - C_{22}\right)\cos\theta\sin^3\theta - C_{26}\sin^4\theta, \tag{14c}$$

$$Q_{22} = C_{22}\cos^4\theta + 4C_{26}\cos^3\theta\sin\theta + 2\left(C_{12} + 2C_{66}\right)\cos^2\theta\sin^2\theta + 4C_{16}\cos\theta\sin^3\theta + C_{11}\sin^4\theta, \tag{14d}$$

$$Q_{26} = C_{26}\cos^4\theta + \left(C_{12} - C_{22} + 2C_{66}\right)\cos^3\theta\sin\theta + 3\left(C_{16} - C_{26}\right)\cos^2\theta\sin^2\theta + \left(C_{11} - C_{12} - 2C_{66}\right)\cos\theta\sin^3\theta - C_{16}\sin^4\theta, \tag{14e}$$

$$Q_{66} = 2\left(C_{16} - C_{26}\right)\cos^3\theta\sin\theta + \left(C_{11} + C_{22} - 2C_{12} - 2C_{66}\right)\cos^2\theta\sin^2\theta + 2\left(C_{26} - C_{26}\right)\cos\theta\sin^3\theta + C_{66}\left(\cos^4\theta + \sin^4\theta\right), \tag{14f}$$

$$Q_{44} = C_{44}\cos^2\theta + 2C_{45}\cos\theta\sin\theta + C_{55}\sin^2\theta, \tag{14g}$$

$$Q_{45} = \left(C_{55} - C_{44}\right)\cos\theta\sin\theta + C_{44}\left(\cos^2\theta - \sin^2\theta\right), \tag{14h}$$

$$Q_{55} = C_{55}\cos^2\theta - 2C_{45}\cos\theta\sin\theta + C_{44}\sin^2\theta, \tag{14i}$$

where θ denotes the orientation angle, and $C_{ij}\ (i, j = 1,2,...,6)$ are the elastic coefficients which can be obtained by the Mori-Tanaka model [13].

3. Energy Method

The strain energy U of the structure can be written as:

$$U = \frac{1}{2}\int_V \left(\sigma_{xx}^{(\mathrm{k})}\varepsilon_{xx} + \sigma_{yy}^{(\mathrm{k})}\varepsilon_{yy} + \sigma_{xy}^{(\mathrm{k})}\gamma_{xy} + \sigma_{xz}^{(\mathrm{k})}\gamma_{xz} + \sigma_{yz}^{(\mathrm{k})}\gamma_{yz}\right)dV\,. \tag{15}$$

Combining Eqs. (7)-(13) yields:

$$U=\frac{1}{2}\int_A\Big(N_x\frac{\partial u}{\partial x}+N_{xy}\frac{\partial u}{\partial y}+N_{xy}\frac{\partial v}{\partial x}+N_y\frac{\partial v}{\partial y}+Q_{xz}\frac{\partial w_s}{\partial x}+Q_{yz}\frac{\partial w_s}{\partial y}$$
$$+\left(S_x-M_x\right)\frac{\partial^2 w_s}{\partial x^2}+\left(S_y-M_y\right)\frac{\partial^2 w_s}{\partial y^2}+2\left(S_{xy}-M_{xy}\right)\frac{\partial^2 w_s}{\partial y\,\partial x}-M_x\frac{\partial^2 w_b}{\partial x^2}$$
$$-M_y\frac{\partial^2 w_b}{\partial y^2}-2M_{xy}\frac{\partial^2 w_b}{\partial y\,\partial x}+P_z\varphi+Q_{xz}\frac{\partial\varphi}{\partial x}+Q_{yz}\frac{\partial\varphi}{\partial y}\Big)dA, \tag{16}$$

where the force, moment, and transverse shear stress resultants may be defined as:

$$\left\{(N_x,N_y,N_{xy}),(M_x,M_y,M_{xy}),(S_x,S_y,S_{xy})\right\}=\sum_{k=1}^{N}\int_{z^{(k-1)}}^{z^{(k)}}\left\{\sigma_{xx},\sigma_{yy},\tau_{xy}\right\}(1,z,f)dz, \tag{17}$$

$$\left\{\left(Q_x,Q_y\right),\left(P_x,P_y\right)\right\}=\sum_{k=1}^{N}\int_{z^{(k-1)}}^{z^{(k)}}\left\{\sigma_{xz},\sigma_{yz}\right\}(g,f)dz, \tag{18}$$

The external work induced by the elastic medium is [14]:

$$W=-\frac{1}{2}\int\underbrace{\left(k_w w-k_g\nabla^2 \mathrm{w}\right)}_{q}wdA, \tag{19}$$

where k_w and k_g are the spring and the shear constants, respectively. The total kinetic energy of the actuator-nanocomposite-sensor structure may be written as:

$$K=\frac{1}{2}\int_A\int_{-h/2}^{h/2}\rho^{(k)}\left(\left(u_1\right)^2+\left(u_2\right)^2+\left(u_3\right)^2\right)dzdA, \tag{20}$$

Based on Hamilton's principle, the motion equations can be derived as follows:

$$\delta u:\ -\frac{\partial N_x}{\partial x}-\frac{\partial N_{xy}}{\partial y}+I_1\frac{\partial^2 u}{\partial t^2}-I_6\frac{\partial^3 w_b}{\partial x\,\partial t^2}+\left(I_7-I_6\right)\frac{\partial^3 w_s}{\partial x\,\partial t^2}=0, \tag{21}$$

$$\delta v:\ -\frac{\partial N_y}{\partial y}-\frac{\partial N_{xy}}{\partial x}+I_1\frac{\partial^2 v}{\partial t^2}-I_6\frac{\partial^3 w_b}{\partial y\,\partial t^2}+\left(I_7-I_6\right)\frac{\partial^3 w_s}{\partial y\,\partial t^2}=0, \tag{22}$$

$$\delta w_b:-\frac{\partial^2 M_x}{\partial x^2}-\frac{\partial^2 M_y}{\partial y^2}-2\frac{\partial^2 M_{xy}}{\partial y\,\partial x}+\Big[I_6\frac{\partial^3 u}{\partial x\,\partial t^2}+I_6\frac{\partial^3 v}{\partial y\,\partial t^2}+I_1\frac{\partial^2 w_b}{\partial t^2}+I_5\frac{\partial^2\varphi}{\partial t^2}$$
$$-N_{ye}\frac{\partial^2 w_b}{\partial y^2}-I_2\frac{\partial^4 w_b}{\partial x^2\partial t^2}-I_2\frac{\partial^4 w_b}{\partial y^2\partial t^2}+\left(I_8-I_2\right)\frac{\partial^4 w_s}{\partial x^2\partial t^2}-N_{xe}\frac{\partial^2 w_b}{\partial x^2}-N_{ye}\frac{\partial^2\varphi}{\partial y^2}$$
$$+\left(I_8-I_2\right)\frac{\partial^4 w_s}{\partial y^2\partial t^2}+I_1\frac{\partial^2 w_s}{\partial t^2}-N_{xe}\frac{\partial^2 w_s}{\partial x^2}-N_{ye}\frac{\partial^2 w_s}{\partial y^2}-N_{xe}\frac{\partial^2\varphi}{\partial x^2}+q=0, \tag{23}$$

$$\delta w_s:\ -\frac{\partial^2 M_x}{\partial x^2}-\frac{\partial^2 M_y}{\partial y^2}-2\frac{\partial^2 M_{xy}}{\partial y\,\partial x}+\frac{\partial^2 S_x}{\partial x^2}+\frac{\partial^2 S_y}{\partial y^2}+2\frac{\partial^2 S_{xy}}{\partial y\,\partial x}-\frac{\partial Q_{xz}}{\partial x}-\frac{\partial Q_{yz}}{\partial y}$$
$$+I_1\frac{\partial^2 w_b}{\partial t^2}+\left(I_2+I_8\right)\frac{\partial^4 w_b}{\partial x^2\partial t^2}+\left(I_3-I_2+2I_8\right)\frac{\partial^4 w_s}{\partial x^2\partial t^2}+\left(I_6+I_7\right)\frac{\partial^3 u}{\partial x\,\partial t^2}$$
$$+I_5\frac{\partial^2\varphi}{\partial t^2}+\left(I_3-I_2+2I_8\right)\frac{\partial^4 w_s}{\partial y^2\partial t^2}+\left(I_6+I_7\right)\frac{\partial^3 v}{\partial y\,\partial t^2}+I_1\frac{\partial^2 w_s}{\partial t^2}-N_{xe}\frac{\partial^2 w_b}{\partial x^2}-N_{ye}\frac{\partial^2\varphi}{\partial y^2}$$
$$-N_{xe}\frac{\partial^2\varphi}{\partial x^2}+\left(I_2+I_8\right)\frac{\partial^4 w_b}{\partial y^2\partial t^2}-N_{xe}\frac{\partial^2 w_s}{\partial x^2}-N_{ye}\frac{\partial^2 w_b}{\partial y^2}-N_{ye}\frac{\partial^2 w_s}{\partial y^2}+q=0, \tag{24}$$

$$\delta\varphi:\ P_z^l-\frac{\partial Q_{xz}}{\partial x}-\frac{\partial Q_{yz}}{\partial y}+I_4\frac{\partial^2\varphi}{\partial t^2}-N_{xe}\frac{\partial^2 w_b}{\partial x^2}-N_{xe}\frac{\partial^2 w_s}{\partial x^2}-N_{xe}\frac{\partial^2\varphi}{\partial x^2}+I_5\frac{\partial^2 w_s}{\partial t^2}$$
$$+I_5\frac{\partial^2 w_b}{\partial t^2}-N_{ye}\frac{\partial^2 w_b}{\partial y^2}-N_{ye}\frac{\partial^2 w_s}{\partial y^2}-N_{ye}\frac{\partial^2\varphi}{\partial y^2}=0, \tag{25}$$

where N_{xe} and N_{ye} are combinations of the mechanical, electrical, and surface forces. Furthermore, the mass moments of inertia can be defined as:

$$\left[I_1\ I_2\ I_3\ I_4\ I_5\ I_6\ I_7\ I_8\right]^{-1}=\sum_{k=1}^{N}\int_{z_{k-1}}^{z_k}\rho\left[1\ z\ z^2\ f\ f^2\ g\ g^2\ zg-f\ -zf\right]^{-1}dz, \tag{26}$$

4. Solution method

The steady state solutions to the governing equations of the plate motion which relate to the simply supported boundary conditions along the edges of the surface electrodes can be assumed as [15]:

$$u(x,y)=u_0\cos\left(\frac{m\pi x}{a}\right)\sin\left(\frac{n\pi y}{b}\right), \tag{27}$$

$$v(x,y)=v_0\sin\left(\frac{m\pi x}{a}\right)\cos\left(\frac{n\pi y}{b}\right), \tag{28}$$

$$w_b(x,y)=w_{b0}\sin\left(\frac{m\pi x}{a}\right)\sin\left(\frac{n\pi y}{b}\right), \tag{29}$$

$$w_s(x,y)=w_{s0}\sin\left(\frac{m\pi x}{a}\right)\sin\left(\frac{n\pi y}{b}\right) \tag{30}$$

$$\varphi(x,y)=\varphi_0\sin\left(\frac{m\pi x}{a}\right)\cos\left(\frac{n\pi y}{b}\right), \tag{31}$$

The uniform compressive edge loading along x and y axes are $N_{xm}=-P$ and $N_{ym}=-kP$, respectively. The in-plane load P is periodic and may be expressed as:

$$P(t)=\alpha P_{cr}+\beta P_{cr}\cos(\omega t), \tag{32}$$

where ω is the frequency of excitation, P_{cr} is the static buckling load, and α and β may be defined as the static and dynamic load factors, respectively. Now motion equations can be written as:

$$\left\{[K-\alpha P_{cr}K_G-\beta P_{cr}\cos(\omega t)K_G][d]+[M][\ddot{d}]\right\}=[0], \tag{33}$$

where $[K]$ is the linear stiffness matrixes and $[M]$ is the mass matrix. In order to determinate the boundaries of the dynamic instability regions, the method suggested by Bolotin [14] is applied. Hence, the components of $\{d\}$ can be written with period $2T$ in the Fourier series as follows:

$$\{d\}=\sum_{k=1,3,\ldots}^{\infty}\left[\{a\}_k\sin\frac{k\omega t}{2}+\{b\}_k\cos\frac{k\omega t}{2}\right], \tag{34}$$

According to this method, the first instability region is usually the most important in the studies of structures. It is due to the fact that the first DIR is wider that other DIRs, and the structural damping in higher regions becomes neutralized [4]. Substituting Eq. (34) into Eq. (33) and setting the coefficients of each sine and cosine as well as the sum of the constant terms to zero yields:

$$\left|\left([K]-P_{cr}\alpha[K_G]\pm P_{cr}\frac{\beta}{2}[K_G]-[M]\frac{\omega^2}{4}\right)\right|=0, \tag{35}$$

By solving the above equation based on the eigenvalue problem, the variation of ω with respect to α can be plotted as DIR.

5. Numerical Results

A computer program is prepared for the numerical solution of the dynamic buckling of the laminated nanocomposite plates resting on an elastic foundation. The material properties of the laminated plates are listed in Table 1 [16].

Table 1. Material properties of the Graphite/Epoxy [16]

Properties	Value
E_{11}	132.38 *GPa*
$E_{22}=E_{33}$	10.76 *GPa*
G_{12}	3.61 *GPa*
$G_{13}=G_{23}$	5.65 *GPa*
$\nu_{11}=\nu_{23}$	0.24
ν_{13}	0.49
ρ	1578 Kg/m^3

In the absence of similar publications in the literature which cover the same scope of the problem, one cannot directly validate the results obtained here. However, the present study could be partially validated based on a simplified analysis suggested by Putcha and Reddy [17] on the buckling analysis of the laminated plates for which SWCNTS as the reinforced and elastic medium were ignored in this paper ($k_w = k_g = C_r = 0$). For this purpose, a simply supported plate is considered with the same material properties as Ref. [17]. The results of the comparison are shown in Table 2. As can be seen, the present results are in good agreement with other works which indicate validation of this study.

Table 2. Comparison of the present work with the published papers

Theory	E_1 / E_2				
	3	**10**	**20**	**30**	**40**
Classic theory, [17]	5.7538	11.4920	19.7120	27.9360	36.160
Mindlin theory, [17]	5.3991	9.9652	15.3510	19.7560	23.4530
Refined theory, [17]	5.3905	9.8336	14.8906	18.8778	22.1194
Present work	5.3918	9.8452	14.9167	18.8769	22.1531

Fig. 2 shows the effect of the number of layers on DIR of the structure. It can be seen that in the symmetric laminated composites (with three number of layers), DIR occurs in higher pulsation frequencies compared with the anti-symmetric ones (with two number of layers). The reason is that the symmetric laminated composite plates are more balance and stable.

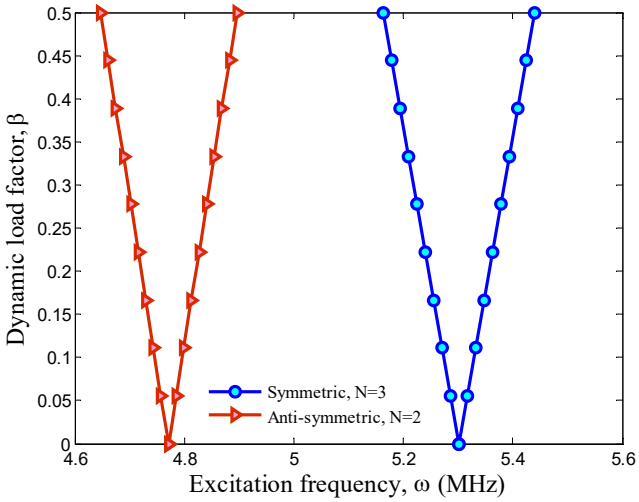

Fig. 2. DIR of the structures with various number of layers

The influence of the orientation type of the layers is studied in Fig. 3. For this purpose, three various types of orientations of the layers are considered as: (0,0,0), (0,90,0), and (45, -45, 45). According to Fig. 3, it can be concluded that the composite structure with the angle-ply orientation of the layers has the highest frequency. Moreover, the composite structure with zero angle orientation of the layers has the lowest frequency.

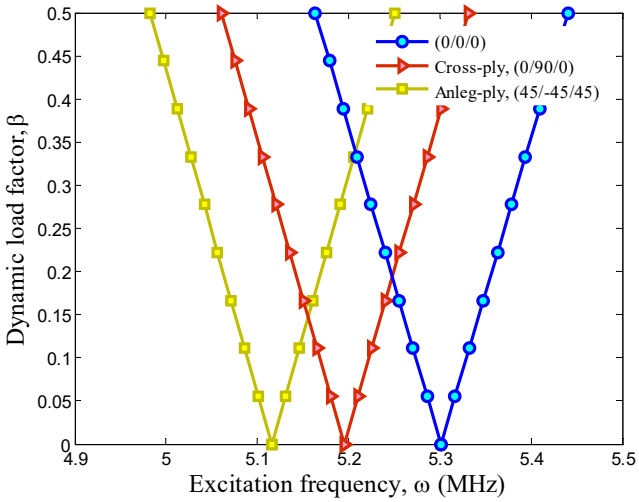

Fig. 3. DIR of the structures with various types of orientation angle of the layers

In Fig. 4, the effect of the SWCNTs volume percentage on DIR is probed. From this figure it can be observed that by increasing the SWCNTs volume percentage, the frequency increases, and DIR is occurred at higher frequencies. Therefore, by increasing the SWCNTs volume percentage, the stiffness of the structure increases.

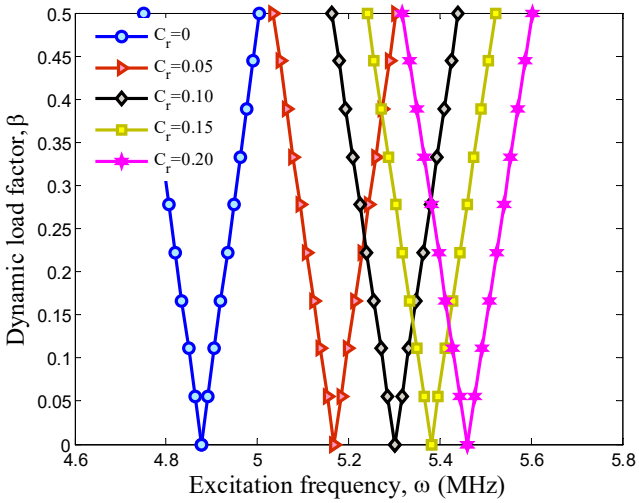

Fig. 4. DIR of the structures with different values of SWCNTs volume percentage versus an axial mode number

The effect of the elastic medium which is modeled by the spring constant of the Winkler medium and the shear layer is studied in Fig. 5. Generally, the existence of the elastic medium causes the increase of the stiffness of the structure, and thereby the frequency increases. The Pasternak medium considers the vertical and shear loads; however, the Winkler medium only considers the vertical ones; therefore, the effect of the Pasternak medium is more than the Winkler medium. According to Fig. 5, the effect of the elastic medium on DIR is significant, and it can be a useful parameter to take the system away from the dynamic buckling condition.

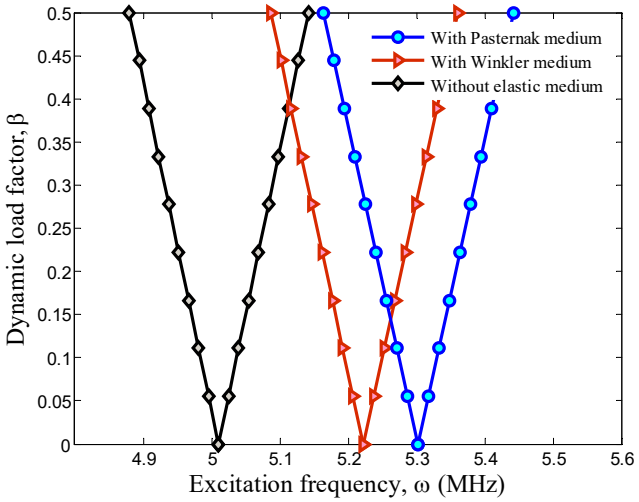

Fig. 5. The effect of the elastic medium on DIR of the structure

Fig. 6 examines the influence of the loading types on DIR of the structure. Two types of loading including the uniaxial (along the *x* axis) and the biaxial (along the *x* and *y* axes) are considered. As it can be found, in the biaxial loading type, the frequency is lower than the axial loading type. The reason is that in the biaxial loading type, the load applied to the edges is higher than the axial loading type; therefore, DIR of the structure occurs sooner.

6. Conclusion

Based on SSDT, the dynamic buckling analysis of an embedded laminated nanocomposite plate was studied in this paper. The structure was surrounded by an elastic medium which generally was simulated by the Pasternak foundation. Using the energy method and Hamilton's principle, the motion equations were derived. In order to obtain DIR, the Navier and Bolotin methods were applied. The effects of the elastic medium, the volume percentage of SWCNTs, the number of layers, and the geometrical parameters of the plate on DIR of the structure were considered. Results indicated that the existence of the elastic medium increases the frequency of the plate. Furthermore, increasing the volume percentage of SWCNTs increased the frequency of the plate, and DIR occured at higher frequencies. In addition, present results are in a good agreement with those reported by Ref. [17]. Finally, it is hoped that the results presented in this paper would be helpful for the study and design of the rectangular laminated

nanocomposite plates.

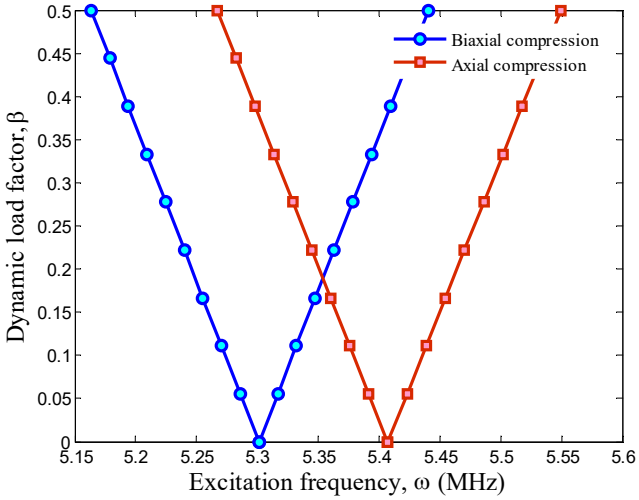

Fig. 6. The effect of the loading type on DIR of the structure

References

[1] Matsunag, H., "Vibration and stability of cross-ply laminated composite plates according to a global higher-order plate theory", Composite Structures, Vol. 48, pp. 231-244, 2000.
[2] Kim, T.W. and Kim, J.H., "Nonlinear vibration of viscoelastic laminated composite plates", International Journal of Solids and Structures, Vol. 39, pp. 2857–2870, 2002.
[3] Malekzadeh, P., Fiouz, A.R. and Razi, H., "Three-dimensional dynamic analysis of laminated composite plates sujected to moving load", Composite Structures, Vol. 90, pp. 105–114, 2009.
[4] Dinis, L.M.J.S., Natal Jorge, R.M. and Belinha, J., "Static and dynamic analysis of laminated plates based on an unconstrained third order theory and using a radial point interpolator meshless method", Computers and Structures, Vol. 89, pp. 1771–1784, 2011.
[5] Honda, Sh., Kumagai, T., Tomihashi, K. and Narita, Y., "Frequency maximization of laminated sandwich plates under general boundary conditions using layerwise optimization method with refined zigzag theory", Journal of Sound and Vibration, Vol. 332, pp. 6451–6462, 2013.
[6] Sahoo, R. and Singh, B.N., "A new shear deformation theory for the static analysis of laminated composite and sandwich plates", International Journal of Mechanical Sciences, Vol. 75, pp. 324–336, 2013.
[7] Heydari, M.M., Kolahchi, R., Heydari, M. and Abbasi, A., "Exact solution for transverse bending analysis of embedded laminated Mindlin plate", Structural Engineering and Mechanics, Vol. 49(5), pp. 661–672, 2014.
[8] Saidi, H., Tounsi, A. and Bousahla, A.A., "A simple hyperbolic shear deformation theory for vibration analysis of thick functionally graded rectangular plates resting on elastic foundations", Geomechanics and Engineering, Vol. 11, pp. 289-307, 2016.
[9] Awrejcewicz, J., Kurpa, L. and Mazur, O., "Dynamical instability of laminated plates with external cutout", International Journal of Non-Linear Mechanics, Vol. 81, pp. 103–114, 2016.
[10] Liang, K., "Koiter–Newton analysis of thick and thin laminated composite plates using a robust shell element", Composite Structures, Vol. 161, pp. 530-539, 2017.
[11] Thai, H.T. and Kim, S.E., "A simple quasi-3D sinusoidal shear deformation theory for functionally graded plates", Composite Structures, Vol. 99, pp. 172-178, 2013.
[12] Reddy, J.N., "A Simple Higher Order Theory for Laminated Composite Plates", Journal of Applied Mechanics, Vol. 51, pp. 745–752, 1984.
[13] Shi, D.L.and Feng, X.Q., "The Effect of Nanotube Waviness and Agglomeration on the elastic Property of Carbon Nanotube-Reinforced Composties", Journal of Engineering Materials and Technology, Vol. 126, pp. 250-270, 2004.
[14] Kolahchi, R., Safari, M. and Esmailpour, M., "Dynamic stability analysis of temperature-dependent functionally graded CNT-reinforced visco-plates resting on orthotropic elastomeric medium", Composite Structures, Vol. 150, pp. 255-265, 2016.
[15] Akhavan, H., Hosseini Hashemi, Sh., Rokni Damavandi Taher, H., Alibeigloo, A. and Vahabi, Sh., "Exact solutions for rectangular Mindlin plates under in-plane loads resting on Pasternak elastic foundation. Part I: Buckling analysis", Computational Material and Science, Vol. 44, pp. 968–978, 2009.
[16] Phung-Van, P., De Lorenzis, L., Thai, Ch.H., Abdel-Wahab, M. and Nguyen-Xuan, H., "Analysis of laminated composite plates integrated with piezoelectric sensors and actuators using higher-order shear deformation theory and isogeometric finite elements", Computational Material and Science, Vol. 96, pp. 495–505, 2015.
[17] Putcha, N.S. and Reddy, J.N., "Stability and natural vibration analysis of laminated plates by using a mixed element based on a refined plate theory", Journal of Sound and Vibration, Vol. 104, pp. 285–300, 1986.